Antitumor Immune Mechanisms of the Anti-Complement Factor H Antibody GT103

Ryan T. Bushey
Duke University
Ruchi Saxena
Duke University
Michael J. Campa
Duke University
Elizabeth B. Gottlin
Duke University
You-Wen He
Duke University
Edward F. Patz, Jr. (patz0002@mc.duke.edu)
Duke University https://orcid.org/0000-0003-3374-1596

Research Article

Keywords: complement factor H, autoantibodies, lung cancer, complement, cancer therapeutics, anti-tumor immunity

Posted Date: November 3rd, 2022

DOI: https://doi.org/10.21203/rs.3.rs-2234932/v1

Abstract

Development of novel therapeutic antibodies that not only kill tumor cells but modulate the adaptive immune response has the potential to produce long term anti-cancer immunity and a durable clinical response. We previously reported the discovery of an anti-complement factor H (CFH) autoantibody in lung cancer patients that were associated with early stage disease and exceptional outcomes. The human monoclonal antibody GT103, produced from a single CFH autoantibody-expressing B cell of a lung cancer patient, recognizes a conformationally distinct epitope on tumor cells, kills tumor cells, and inhibits tumor growth in animal studies. Recent experiments have shown that GT103 restructures the tumor microenvironment and initiates a robust antitumoral adaptive immune response. The current study further elucidates several mechanisms by which GT103 kills tumor cells and drives the immune program. Here we show GT103 has specificity for tumor cells without binding to native soluble CFH or normal tissues. GT103 causes complement C3 split product deposition on tumor cells *in vitro* and *in vivo,* triggers antibody-dependent cellular phagocytosis, and increases translocation of the danger associated molecular pattern molecule calreticulin to the plasma membrane. We also demonstrate that GT103 causes B cell activation and that GT103 antitumor activity *in vivo* is B cell dependent. The complex mechanism of GT103, a tumor specific antibody that kills tumor cells and stimulates an immune response, supports further development of this human-derived antibody as a novel therapeutic option for patients with lung cancer.

Introduction

Immune checkpoint inhibitors have made a significant impact on the treatment of cancer; however, they are only effective in a minority of patients (1). A more comprehensive understanding of how to initiate and drive a robust antitumor immune response will provide valuable insight into developing novel therapeutic strategies. We suggest that for a durable clinical response, a drug must not only target and kill tumor cells, but also engage adaptive immunity. Tumors are composed of a variable mixture of tumor and host cells, and by studying the native immune responses of patients that do exceptionally well we may obtain invaluable information about mechanisms by which to create effective antitumor immunity.

Prior studies have shown that tumor rejection initiated by autoantibodies can promote an adaptive immune response (2,3). In a search for autoantibodies correlated with a more favorable cancer phenotype, we found that patients with early-stage non-small cell lung cancer (NSCLC) had a significantly higher incidence of anti-complement factor H (CFH) autoantibodies than those with more advanced stage disease (4). These autoantibodies were also associated with increased time to recurrence in stage I NSCLC patients (5). CFH is a regulatory protein that protects host cells from destruction by the alternative pathway of complement-dependent cytotoxicity (CDC) but it is also hijacked by tumor cells as an evasive strategy to counter antitumor immunity (6-11). We cloned the genes encoding anti-CFH autoantibodies from single antigen-specific B cells of NSCLC patients and are developing one of them, GT103 (formerly mAb7968), as a therapy for cancer (12). GT103 recognizes an altered conformational epitope of CFH on tumor cells, kills tumor cells *in vitro* by CDC, and inhibits tumor growth and metastasis *in vivo* while

having no observable effect on normal cells (12-14). More recently, Saxena et al. (15) found that GT103 promotes the formation of an antitumor microenvironment characterized by reduced populations of immunosuppressive T regulatory cells and myeloid derived suppressor cells and increased populations of antigen-specific CD4+ and CD8+ T cells.

The purpose of the current study was to further elucidate the mechanisms by which GT103 targets and kills tumor cells. We report the following mechanistic findings: First, GT103 specifically binds to tumor tissues but not native soluble CFH or normal tissues. Second, as a result of inducing CDC of tumor cells, GT103 causes translocation of the immunogenic damage associated molecular pattern (DAMP) molecule calreticulin to the plasma membrane. Third, by virtue of binding to tumor cells in the absence of complement, GT103 directly promotes their antibody-dependent cellular phagocytosis (ADCP). Fourth, GT103-induced CDC results in the release of bioactive complement split products known to bind to receptors on B cells. Fifth, GT103 promotes B cell activation *in vitro* and *in vivo* and the antitumor growth activity of GT103 depends on B lymphocytes. The multi-pronged mechanism of GT103, combined with an extraordinary safety profile in a phase 1b clinical trial, supports GT103 as a novel treatment for lung cancer.

Materials And Methods

Tumor growth in mice

As described in Saxena et al. (15), six- to eight-week-old female C57BL/6 mice were implanted s.c. in the right flank with 2.0×10^5 CMT167 lung tumor cells. One week after inoculation, mice were treated for 2 weeks with murine GT103 (mGT103 - 200 µg/mouse i.p.) or a control solution (200 µg/mouse murine IgG2 [mIgG2] i.p.) three times weekly. Murine GT103 has the identical complementarity determining region as human GT103, and the autoantibody from which human GT103 was derived, set in a murine IgG2 framework.

For the B cell ablation experiment, mice were injected with anti-CD20 (Biolegend) (250 µg i.v.) three days prior to tumor inoculation. B cell-depleted and nondepleted mice were inoculated s.c. with 2.5×10^5 CMT167 cells. When tumors were palpable, mice in each group were randomized and dosed three times a week with either control mIgG2 (100 µg i.p.) or mGT103 (200 µg i.p.). Tumor volume was plotted as mean ± SEM for each treatment group. For all animal experiments, mice were euthanized according to protocols approved by the Duke University Institutional Animal Care and Use Committee.

Immunofluorescence staining of frozen mouse tissues with GT103

Mouse tumor and kidney specimens used in this study were from the vehicle-treated arm of a CMT167 tumor growth study. After the mice were sacrificed, tumors or kidneys were frozen, after which they were cut into 7 µm sections and placed on slides for immunofluorescence analyses. For staining with GT103, sections were fixed in 4% paraformaldehyde (PFA) for 20 min at room temperature and blocked in 5% goat serum (Sigma G9023)/PBS (ThermoFisher 10010-023) with 0.5% Tween (PBST)

for 1 hr at room temperature. The samples were incubated with human GT103, or an IgG3 control antibody (Dendritics DDXCHO3P), at 5 or 50 µg/ml overnight at 4°C in 1% goat serum/PBST, followed by an Alexa Fluor 488 goat anti-human secondary antibody (Invitrogen A11013) at 10 µg/ml in 1% goat serum/PBST for 2 hrs at room temperature. Slides were washed 4x with PBST following the primary and secondary antibody incubations. Hoechst DNA stain (ThermoFisher 62249) was used at 1 µg/ml for 5 mins at room temperature. Prolong Gold (ThermoFisher P10144) was used as the mountant. Sections were stained with secondary antibody alone as a negative control. All microscopy was performed using a Zeiss Axio Imager Widefield Fluorescent Microscope in the Duke Light Microscopy Core Facility.

Immunofluorescence staining of human lung tumor and normal human lung with GT103

The use of human specimens in this study was approved by the Duke Health Institutional Review Board. Formalin-fixed paraffin-embedded (FFPE) normal lung and human lung tumor tissue from a tissue microarray (TMA) were cut into 7 µm sections and placed on slides. The TMA had 33 usable lung tumor spots from individuals with NSCLC. There were 19 females (10 anti-CFH autoantibody positive and 9 autoantibody negative) and 14 males (6 autoantibody positive and 8 autoantibody negative), with all stages of NSCLC represented. Anti-CFH autoantibody status was determined by serum ELISA as previously described (5). Samples were rehydrated using a xylene and ethanol gradient, and antigen retrieval was performed using a citrate buffer (Sigma C9999) and heating in a microwave oven. Blocking was done in 5% goat serum/PBST for 1 hr at room temperature. Murinized (IgG2a) GT103 was used at 50 µg/ml in 1% goat serum/PBST overnight at 4°C. A negative control murine IgG2a antibody (Bio X Cell BP0085) was used at the same concentration. An Alexa Fluor 488 goat anti-mouse secondary antibody (Invitrogen A11001) was used at 10 µg/ml in 1% goat serum/PBST for 2 hrs at room temperature. Washes after primary and secondary antibody incubations, DNA staining, mounting, and imaging were performed as described above.

Competition ELISA

We have previously determined the epitope to which GT103 binds (13). A biotinylated GT103 epitope-containing peptide (GPPPPIDNGDITSFPGGG-K(biotin); epitope underlined), at 2 µg/ml in Ca^{++}- and Mg^{++}-free Dulbecco's phosphate-buffered saline (DPBS, ThermoFisher), was immobilized in the wells of an ELISA plate precoated with NeutrAvidin (ThermoFisher) by overnight incubation at 4°C. The wells of the plate were then washed 4 times with PBST and incubated at room temperature for 90 min with GT103 (0.25 to 0.0039 µg/ml in 2-fold dilutions) either alone or previously incubated with CFH (50 µg/ml) for 0 or 1 h at room temperature, or 24 h at 4°C. After washing as described, bound GT103 was detected with an anti-human IgG (γ-chain specific)-HRP conjugate (Chemicon AP504P). After washing as before, 1-Step ABTS (ThermoFisher) was added and color development was quantified by absorbance at 405 nm.

Calreticulin plasma membrane expression following GT103 treatment

H460 (human large cell lung cancer) and A549 (human lung adenocarcinoma) cells were grown in RPMI + FBS until 75% confluent. Cells were rinsed 3x with DPBS, then treated with 10% NHS and human

GT103 or control antibody at 200 µg/ml for 2 hrs at 37°C. Doxorubicin (Sigma D1515) was used at 25 µM as a positive control. Cells were washed 3x with DPBS and detached with Versene. Plasma membrane protein was isolated using a plasma membrane protein extraction kit (101 Bio P503). Five µg of plasma membrane protein was loaded per lane in a Western blot. Blocking was done using 5% milk/PBST, and the blot was probed with an anti-calreticulin antibody (ThermoFisher PA3-900) at a 1:1000 dilution for 2 hrs at room temperature in 5% milk/PBST. The membrane was probed with an anti-rabbit HRP secondary antibody at a 1:10000 dilution in 5% milk/PBST for 1 hr at room temperature. The membrane was washed 4x with PBST following the primary and secondary antibody incubations. The blot was stripped and probed with a beta-actin antibody (R&D MAB8929) as a loading control. The experiment was repeated and whole cell lysate, rather than plasma membrane protein, was isolated after lysing cells with M-PER and probed with the anti-calreticulin antibody as described for the plasma membrane protein.-

Immunofluorescence staining of frozen mouse tumors with anti-calreticulin antibody

Frozen CMT167 tumor sections were fixed with 4% PFA for 15 minutes. Blocking was done in 5% goat serum/PBST for 1 hr at room temperature. An anti-calreticulin antibody (ThermoFisher PA3-900) was used at a 1:75 dilution in 1% goat serum/PBST. An Alexa Fluor 488 goat anti-rabbit secondary antibody (Invitrogen A11008) was used at 10 µg/ml in 1% goat serum/PBST for 2 hrs at room temperature. Washes after primary and secondary antibody incubations, DNA staining, mounting, and imaging were performed as described above. The mean fluorescence intensity (MFI) of calreticulin was quantified using FIJI/ImageJ. The MFI of calreticulin was divided by the MFI of DNA stain for each spot to account for differences in the number of cells in each image.

C3b/iC3b deposition on human lung cancer cell lines following GT103 treatment

H460 or A549 human lung cancer cells were plated at concentration of 10^4 cells/well in a 96 well plate in RPMI (ThermoFisher 11875-093) + 10% FBS. The following day, cells were washed 3x with Dulbecco's Phosphate Buffered Saline (DPBS, ThermoFisher 14190-144) and treated with antibody and normal human serum (NHS, Complement Technology) as a source of complement. Human GT103 or a matched IgG control antibody were used at 200 µg/ml, while NHS was used at 10% of the final reaction volume. Cells were treated in 50% serum free RPMI and 50% 1x Veronal buffer (Lonza 12-624E). NHS was heat inactivated for 30 min at 56°C as a negative control, and in some experiments C1q depleted serum or Factor B depleted serum (Complement Technology) were also used at 10% final dilution. The cells were treated for 24 hrs in a 37°C incubator. The following day, cells were detached with Versene solution (ThermoFisher 15040-066), washed 3x with DPBS, and stained with allophycocyanin (APC) labeled anti-complement C3b/iC3b antibody (Biolegend 846105) per the manufacturer's protocol. Samples were run on a FACSCanto analyzer in the Duke Cancer Institute flow cytometry core facility.

C1q surface binding to a human lung cancer cell line following GT103 treatment

H460 cells were grown in culture, rinsed 3x in DPBS, and detached with Versene. $2.5x10^5$ cells were used in each condition, and each condition was run in duplicate. Cells were treated with 10% C4-depleted serum (Complement Technology) in 50% RMPI and 50% Veronal buffer. C4-depleted serum was used to prevent complement mediated lysis induced by GT103 from occurring. Human GT103 and a matched IgG control antibody were used at 200 µg/ml, and cells were treated for 2 hrs at 37°C. In addition to GT103, a $F(ab')_2$ fragment of human GT103 was cloned and purified at the Duke Human Vaccine Institute and used in this experiment. The $F(ab')_2$ was used as additional control as it lacks CH2 in the Fc segment of the antibody to which C1q binds. Following treatment, cells were washed 3x with DPBS and stained with a C1q-FITC antibody (Thermo Fisher PA5-16601) per the manufacturer's recommended protocol. Cells were washed 3x with DPBS and run on the FACSCanto analyzer.

Immunofluorescence staining of frozen mouse tumor with anti-C3b/iC3b/C3c antibody

CMT167 tumor sections were fixed in acetone for 5 minutes at room temperature and treated with 3% H_20_2/methanol for 10 minutes at room temperature to block endogenous peroxidases. Blocking was done in 5% goat serum/PBST for 1 hr at room temperature. An anti-C3b/iC3b/C3c antibody (Hycult HM1065) was used at 1:25 dilution in 1% BSA/PBS. An Alexa Fluor 488 goat anti-rat secondary antibody (Invitrogen A11006) was used at 10 µg/ml in 1% goat serum/PBST for 2 hrs at room temperature. Washes after primary and secondary antibody incubations, DNA staining, mounting, and imaging were performed as described above.

Detection and quantification of C3d fragments in GT103 treated CMT167 tumors

CMT167 tumor lysates were made using M-PER (ThermoFisher 78501) from five GT103 treated mice and five control mice. 15 µg of protein from each tumor lysate was loaded per lane. The blot was blocked with 5% milk/PBST for 1 hr at room temperature and probed with an anti-C3d antibody (R&D Systems AF2655) at 0.2 µg/ml in 5% milk/PBST for 2 hrs at room temperature. The blot was probed with a rabbit anti-goat HRP antibody (Santa Cruz sc2768) at a 1:5000 dilution in 5% milk/PBST for 1 hr at room temperature. The blot was washed 4x with PBST following the primary and secondary antibody incubations. C3d and C3dg fluorescence was measured using Image Lab Software (BioRad).

Macrophage mediated ADCP following GT103 treatment

PBMCs were isolated from a normal donor blood using Ficoll separation. As described in a previous publication (16), PBMCs at a concentration of $1x10^6$ cells/ml were plated in medium containing RMPI + 10% FBS, 8% NHS, 20 mM HEPES (ThermoFisher15630080), and 50 ng/ml hm-CSF (Cell Signaling 8929). PBMCs were grown in this medium for 5 days to allow the adherent cell population to differentiate into macrophages. Following this period, macrophages were detached with cold DPBS and labeled with Cell Trace Violet (ThermoFisher C34571). H460 cells were labeled with CFSE (ThermoFisher C34554). Labeled macrophages were suspended in RPMI + 10% FBS at a concentration of $1x10^6$ cells/ml, while labeled H460 cells were suspended in the same medium at a concentration of $2x10^6$

cells/ml. A co-incubation step followed, where 50 µl of labeled tumor cells and 100 µl of labeled macrophages were added to the wells of a 96 well plate. Human GT103 or a matched IgG control antibody were added at 250 µg/ml. The co-incubation was done for 4 hrs in a 37°C incubator. Cells were detached with Versene and run on the FACSCanto analyzer. Each condition was run in duplicate, and phagocytosis was determined by calculating the percentage of double positive cells.

GT103-induced B cell Syk kinase phosphorylation

H460 lung cancer cells were plated at $2x10^4$ cells/well in a 96 well plate in RPMI + FBS media. The following day, cells were washed 3x with DPBS and treated with antibody and NHS. Human GT103 or a matched IgG control antibody were used at 200 µg/ml, while NHS was used at 10% of the final reaction volume. The cells were treated with antibody and serum for 1 hr in a 37°C incubator. PMBCs from a normal donor were isolated using a Ficoll gradient, and B cells were isolated using an isolation kit (Miltenyi 130-091-151). 8×10^4 B cells were added to each well of the 96 well plate containing tumor cells, and the cells were co-incubated for 24 hrs in a 37°C incubator. For western blot analysis of phosphorylated Syk, cells were detached from the wells using Versene and protein was isolated using M-PER. 15 µg of protein from each co-incubation condition was loaded per lane. The blot was blocked with 5% milk/PBST for 1 hr at room temperature and probed with an anti-phospho-Syk antibody (ThermoFisher MA5-14918) at a 1:1000 dilution in 5% milk/PBST overnight at 4°C. The blot was probed with an anti-rabbit HRP secondary antibody (Thermo 65-6120) at 1:10000 dilution in 5% milk/PBST for 1 hr at room temperature. The blot was washed 4x with PBST following the primary and secondary antibody incubations. For flow cytometry experiments investigating phosphorylation of Syk, heat inactivated NHS and B cells not co-cultured with tumor cells were used as additional controls. Following co-incubation, cells were detached and stained with the anti-phospho-Syk antibody at 1:200 dilution using a Biolegend intracellular staining protocol. Cells were stained for 20 min at 4°C, washed, and stained with an anti-rabbit BV-421 secondary antibody (Biolegend 406410) at 1:50 dilution for 20 min at 4°C. Each condition was run in triplicate. B cells were gated based on size difference from tumor cells when samples were run on the FACSCanto analyzer.

Statistical Analyses

An unpaired, two-tailed Student's t-test was used for all analyses in which a p-value was derived.

Data Availability Statement

The data generated in this study are available upon request from the corresponding author.

Results

GT103 has specificity for tumor tissue

We previously reported that GT103 causes CDC of tumor cells *in vitro* and postulated that its tumor specificity *in vivo* was due to an inhibitory effect on tumor growth while not affecting normal tissues (12). In this study, we further probed GT103 binding specificity to tumors compared to native, soluble CFH by competition assay, and to normal tissues by immunofluorescence. Using GT103 as a probe at concentrations of 5 and 50 µg/ml, we detected fluorescence in CMT167 tumor tissue while there was no detectable fluorescence in normal mouse kidney (**Fig. 1A-D**). Minimal fluorescence was observed with anti-human secondary antibody alone (data not shown).

To further investigate GT103 tumor specificity in human tissues, immunofluorescence was performed with a murine version of GT103 (mGT103) as primary antibody on TMA sections containing lung tumor tissues from 33 NSCLC patients and normal lung tissue. Variability in GT103 fluorescence was observed in tumor tissues but essentially no detectable fluorescence was observed in normal human lung tissue (**Fig. 1E-H**). No fluorescence was observed with anti-mouse secondary antibody alone (data not shown).

In addition to exploring the binding of GT103 to human tumor or normal tissue, we were also interested in determining if GT103 could interact with fluid-phase CFH as it exists in the blood. To this end, we performed an ELISA designed to gauge the ability of purified soluble CFH to compete with an GT103 epitope-containing peptide for binding to GT103. After pre-incubation of GT103 with a 12,800-fold molar excess of CFH for up to 24 h, no detectable effect on the binding of GT103 to immobilized epitope-containing peptide was observed (**Fig. 1I-J**).

GT103 increases calreticulin plasma membrane expression

We previously reported that GT103 causes cell death by CDC with release of the soluble complement activation products C3a and C5a (12). Complement activation, including the release of these pro-inflammatory cytokines, has been reported to increase the presence of DAMPs (17). Calreticulin, a canonical DAMP, is upregulated during cellular stress and, when translocated to the cell surface, promotes phagocytosis and antigen processing by immune cells (18,19). To determine whether GT103 treatment causes either upregulation of calreticulin or its translocation to the cell surface, H460 and A549 lung cancer cells were treated *in vitro* with GT103, control IgG, or doxorubicin, a known inducer of calreticulin translocation (19). Plasma membrane protein was isolated, and GT103 and doxorubicin were each found to increase plasma membrane calreticulin by approximately 2-fold over the IgG control in both cell lines **(Fig. 2A-B)**. No change in calreticulin expression was detectible by western blot in whole cell lysates from GT103 treated cells. When CMT167 tumors from animal studies were probed with a calreticulin antibody, mGT103-treated CMT167 tumors **(Fig. 2C-D)** exhibited higher calreticulin immunofluorescence than control-treated CMT167 tumors **(Fig. 2E-F)**; green fluorescence values in the representative sections shown in **Fig. 2C-F** were 1.07 and 1.29 for mGT103-treated tumors vs. 0.42 and 0.54 for control-treated tumors.

We then wanted to determine if a similar pattern was seen in human lung cancer samples from patients with and without the anti-CFH autoantibody. By analogy of GT103 with the anti-CFH autoantibody from which it was derived, we hypothesized that tumors from CFH autoantibody-positive NSCLC patients

would have higher calreticulin levels than tumors from CFH autoantibody-negative NSCLC patients. We probed a microarray containing 33 sections of human lung tumors and quantitated calreticulin immunofluorescence; examples of two such sections are shown in **Fig. 2G-H**. While there was variability among the human samples overall, and overlap between the two populations, there was a significantly higher calreticulin immunofluorescence in the anti-CFH autoantibody-positive tumors than tumors from anti-CFH autoantibody-negative individuals **(Fig. 2I)** (p=0.002).

GT103 causes deposition of C3 fragments on tumor cells and in tumor tissues via activation of the classical complement pathway

We have previously shown that GT103 causes complement activation *in vitro*; treatment of lung tumor cells with GT103 causes release of C3a, C5a, and deposition of C5b-9 (12). Here we determined whether GT103 causes an increase in C3b/iC3b deposition on tumor cells both *in vitro* and *in vivo.* While C3b deposition initiates the cascade that ultimately results in the formation of the membrane attack complex, three antigen-linked proteolytic degradation fragments of C3b – iC3b, C3dg, and C3d – bind to complement receptor 2 (CR2) via their common, exposed C3d moiety (20-24). Binding of these antigen-linked C3d-displaying fragments to CR2 receptors on B cells and follicular dendritic cells (DCs) results in activation of B cells and augmentation of B cell affinity maturation by the follicular DCs displaying these antigens in germinal centers (25). GT103 caused a significant increase in C3b/iC3b deposition on the surface of A549 human lung cancer cells compared to a control IgG (p=0.001) (**Fig. 3A**). GT103 also caused a significant increase in C3b/iC3b deposition on the surface of human lung cancer H460 cells compared to control antibody (p=0.03) (**Fig. 3B**).

Sera depleted of Factor B and C1q were used to further investigate the pathway by which GT103 causes C3b/iC3b deposition on the H460 tumor cell surface: Factor B-depleted serum blocks alternative complement pathway activation, while C1q-depleted serum blocks classical pathway activation (26). Factor B-depleted serum combined with GT103 caused C3b/iC3b deposition similar to that caused by nondepleted NHS (p=0.25), while C1q-depleted serum with GT103 caused significantly lower C3b/iC3b on the H460 cell surface (p=0.01) (**Fig. 3B**). These results suggest that even though CFH regulates the alternative complement pathway, GT103 bound to CFH activates the classical complement pathway, in keeping with our previous report that CDC by GT103 primarily relies on the classical pathway (27).

The dependence of GT103-mediated C3b deposition and CDC on C1q suggested that C1q binding to tumor cells should be higher in the presence of GT103 than in its absence. To test this hypothesis, H460 cells were treated with GT103, control IgG, or a $F(ab')_2$ fragment of GT103 in the presence of C4-depleted serum (used to prevent complement mediated lysis induced by GT103 and preserve cell integrity). GT103 caused a significant increase in C1q binding to the cell surface compared to IgG control antibody (p=0.02) or the $F(ab')_2$ fragment (p=0.008) (**Fig. 3C**).

Following these *in vitro* results, we asked whether activated C3 products could be detected in CMT167 tumors in mice treated with mGT103. An immunofluorescent signal was clearly detected in CMT167

tumors from mGT103 treated mice **(Fig. 3D-E)** with a primary antibody that detects C3b, iC3b, and C3c, while no detectable C3 fragments were detected in control treated mice **(Fig 3F-G)**. No fluorescence was observed when secondary antibody was used alone (data not shown). To differentiate C3b products that display the CR2 ligand C3d from those that do not, we assayed tumor lysates by western blot with a C3d-specific antibody that detects both C3dg and C3d (data not shown). Mean levels of C3dg and C3d in CMT167 tumors of mGT103-treated mice were ~2-fold higher than those of control-treated mice (mean chemiluminescence intensity for C3dg: 113.8 vs. 69.7; C3d: 49.0 vs. 21.6). These experiments support previous observations that GT103 causes increased complement activation and suggest the intriguing possibility that GT103 treatment of tumor cells can cause activation of immune cells via the production of molecules that bind to the CR2 receptor.

GT103 promotes ADCP

The fact that GT103 induces CDC by the classical pathway implies that the antibody stably binds to its target on the cell surface, enabling Fc-C1q interaction. Therefore, we hypothesized that the Fc portion of GT103 bound to a tumor cell could also interact with the Fc receptor on a phagocytic cell, enabling ADCP of the tumor cell. We tested this hypothesis, with antibody-bound H460 tumor cells acting as the target and macrophages acting as the effector cell. GT103 caused significantly increased phagocytosis (p=0.002) of H460 cells, compared to IgG control antibody **(Fig. 4)**.

GT103 activates B cells through Syk kinase phosphorylation

Among many downstream effects of complement activation, the interaction between complement C3 split products and CR2 on B cells links complement activation and humoral immunity through B cell activation (20). Co-culture experiments were performed to determine whether GT103 mediated complement activation could have an activating effect on B cells. Phosphorylation of Syk, a tyrosine kinase, has been reported to be C3 fragment dependent and be crucial for B cell activation (20,28). When tumor cells were treated with GT103 and NHS as a source of complement, B cells were found to have significantly higher levels of phosphorylated Syk by western blot **(Fig. 5A)** and flow cytometry **(Fig. 5B)** compared to tumor cells treated with control antibody (p=0.04).

GT103 activity *in vivo* is dependent on B cells

Saxena et al. (15) showed that one of the top immunologically-related pathways upregulated by GT103 in CMT167 mouse tumors was that related to B cell receptor signaling. We hypothesized B cells are required for GT103 activity. To directly test this hypothesis, we performed an experiment in which B cells were depleted with an anti-CD20 antibody, CMT167 tumors were initiated, then mice were treated with mGT103 or subclass-matched control IgG2. Anti-CD20 antibody depleted B cells efficiently (**Fig. 6A**). In the absence of B cells, GT103 efficacy was abolished, demonstrating that B cells are essential for its antitumor activity (**Fig. 6B**).

Discussion

In a search for antibodies associated with a favorable outcome in NSCLC patients, we discovered an autoantibody to CFH (4,5). We have since found that GT103, a monoclonal antibody derived from this autoantibody, inhibits tumor growth and has many immune-stimulatory effects (12,15), but the mechanisms by which it exerts these effects have been unclear. Here we have focused on determining the effects of GT103 on immunity brought about by its activation of the complement system.

The complement system is an essential part of innate immunity that eliminates pathogens and altered host cells, and when activated has wide-ranging immunological effects (29). In a cascade of proteolytic cleavages starting from the parent C3 molecule, complement “split” products are released and terminal MAC components are deposited in the membrane. Among the split products are the potent pro-inflammatory anaphylatoxins C3a and C5a and the biologically active degradation products of C3b. Complement activation also acts as a bridge between the innate and adaptive immune systems since complement receptors are expressed on immune cells, including CR1 and CR2 on B cells and follicular DCs and CR3 on cells of the myeloid lineage in mice, with CR1 and CR2 expressed on additional cell types in humans (30).

In order to prevent unwanted damage to normal cells, the complement system must be tightly regulated (26). CFH is one of multiple regulatory proteins that protect normal host cells from CDC and is also overexpressed by, and protects tumor cells (31,32) including those in cancers of the lung, breast, ovaries, and colon (6,11,33-35). Targeting CFH not only causes increased tumor cell cytotoxicity but may also more broadly stimulate antitumor immunity. Indeed, Saxena et al. (15) have shown that GT103, an antibody that targets CFH in a tumor cell-specific manner, has multiple effects on antitumor immunity, downregulating immunosuppressive cell types and stimulating the production of antigen-specific CD4+ and CD8+T lymphocytes.

In this study we investigated mechanistic links between complement activation by GT103 and the modulation of adaptive immunity. First, we showed that in both mouse and human samples, GT103 does not bind to native, soluble CFH and has specificity for tumor tissue, which suggests this antibody will have an exceptional safety profile as a therapeutic without off-target effects. Tumor specificity is the key to unleashing a local antitumor immune response and the basis of this specificity may lie in the fact that GT103 recognizes a cryptic epitope in CFH (12) that we have proposed is exposed in the tumor environment. We previously found that GT103 kills tumor cells by inducing the classical pathway of CDC, and to a lesser extent, the alternative pathway (27). Using depleted sera lacking the capacity to carry out each pathway we showed that GT103 increased deposition of C3 fragments on tumor cells via the classical pathway; in addition, GT103, but not its $F(ab')_2$ fragment, increased binding of C1q to tumor cells. GT103-bound tumor cells also proved to be a target for macrophage-mediated ADCP, presumably through the recognition of immune complexes on the tumor cell surface by Fc receptors on macrophages.

Our data suggests that GT103-mediated CDC could potentially also lead to phagocytosis by a second mechanism: inducing translocation of surface exposed calreticulin to the plasma membrane during the

process of immunogenic cell death. CDC of tumor cells has been described as a programmed or “necroptotic” cell death and not a simple osmotic lysis (36-38). Both apoptosis and necroptosis are forms of immunogenic cell death, one marker of which is the translocation of calreticulin to the plasma membrane (39,40). Plasma membrane calreticulin triggers engulfment of the dying cell by macrophages and DCs, followed by cross-presentation of cellular antigens (18,19,41), thus increasing the susceptibility of the cell to phagocytosis.

Our results also suggest that GT103-mediated CDC activates B cells *in vivo* by generating C3 split products in the tumors of GT103-treated tumor bearing mice, including increased C3d and C3dg. These molecules have profound effects on the local immune system (20). A recent publication confirmed the link between complement split products and a lowered activation threshold of B cells in an E0771 cell inoculated mouse model (42). Furthermore, we showed a direct link between GT103-mediated complement activation and B cell activation through phosphorylated Syk. This result is in keeping with the results of Saxena et al. (15) that showed that GT103 enhanced expression of genes in the B cell activation pathway *in vivo*. Finally, we showed that B cells are required for inhibition of tumor growth by GT103 *in vivo*.

GT103 is a novel antibody that holds tremendous promise in treating lung cancer and potentially other solid tumors that use a similar protective mechanism. By replicating the CFH autoantibodies found in early-stage lung cancer patients with a favorable outcome, GT103 recognizes a unique tumor specific conformational target and has a novel mechanism of action. In this report, we highlight the specificity of GT103 and the multifarious mechanisms by which GT103-mediated complement activation initiates the development of an adaptive immune response. In future studies, clinical trial samples will enhance our efforts to discover potential biomarkers for GT103 efficacy, and also whether we can predict which patients will benefit the most from GT103 treatment.

References

1. Schoenfeld AJ, Hellmann MD. Acquired Resistance to Immune Checkpoint Inhibitors. Cancer cell 2020;37(4):443–55 doi 10.1016/j.ccell.2020.03.017.
2. Carmi Y, Engleman EG. Tumor-binding antibodies and tumor immunity. Oncotarget 2015;6(34):35129–30 doi 10.18632/oncotarget.4889.
3. Carmi Y, Spitzer MH, Linde IL, Burt BM, Prestwood TR, Perlman N, *et al.* Allogeneic IgG combined with dendritic cell stimuli induce antitumour T-cell immunity. Nature 2015;521(7550):99–104 doi 10.1038/nature14424.
4. Amornsiripanitch N, Hong S, Campa MJ, Frank MM, Gottlin EB, Patz EF, Jr. Complement factor H autoantibodies are associated with early stage NSCLC. Clin Cancer Res 2010;16(12):3226–31 doi 10.1158/1078 – 0432.CCR-10-0321.
5. Gottlin EB, Campa MJ, Gandhi R, Bushey RT, Herndon 2nd JE, Patz Jr. EF. Prognostic significance of a complement factor H autoantibody in early stage NSCLC. Cancer Biomarkers 2022;34(3):385–92.

6. Ajona D, Hsu YF, Corrales L, Montuenga LM, Pio R. Down-regulation of human complement factor H sensitizes non-small cell lung cancer cells to complement attack and reduces in vivo tumor growth. J Immunol 2007;178(9):5991–8.
7. Horl S, Banki Z, Huber G, Ejaz A, Windisch D, Muellauer B, *et al.* Reduction of complement factor H binding to CLL cells improves the induction of rituximab-mediated complement-dependent cytotoxicity. Leukemia 2013;27(11):2200–8 doi 10.1038/leu.2013.169.
8. Winkler MT, Bushey RT, Gottlin EB, Campa MJ, Guadalupe ES, Volkheimer AD, *et al.* Enhanced CDC of B cell chronic lymphocytic leukemia cells mediated by rituximab combined with a novel anti-complement factor H antibody. PLoS One 2017;12(6):e0179841 doi 10.1371/journal.pone.0179841.
9. Junnikkala S, Jokiranta TS, Friese MA, Jarva H, Zipfel PF, Meri S. Exceptional resistance of human H2 glioblastoma cells to complement-mediated killing by expression and utilization of factor H and factor H-like protein 1. J Immunol 2000;164(11):6075–81.
10. Varsano S, Rashkovsky L, Shapiro H, Ophir D, Mark-Bentankur T. Human lung cancer cell lines express cell membrane complement inhibitory proteins and are extremely resistant to complement-mediated lysis; a comparison with normal human respiratory epithelium in vitro, and an insight into mechanism(s) of resistance. Clinical and experimental immunology 1998;113(2):173–82.
11. Wilczek E, Rzepko R, Nowis D, Legat M, Golab J, Glab M, *et al.* The possible role of factor H in colon cancer resistance to complement attack. Int J Cancer 2008;122(9):2030–7.
12. Bushey RT, Moody MA, Nicely NL, Haynes BF, Alam SM, Keir ST, *et al.* A Therapeutic Antibody for Cancer, Derived from Single Human B Cells. Cell Rep 2016;15(7):1505–13 doi 10.1016/j.celrep.2016.04.038.
13. Campa MJ, Gottlin EB, Bushey RT, Patz EF, Jr. Complement Factor H Antibodies from Lung Cancer Patients Induce Complement-Dependent Lysis of Tumor Cells, Suggesting a Novel Immunotherapeutic Strategy. Cancer Immunol Res 2015;3(12):1325–32 doi 10.1158/2326–6066.CIR-15-0122.
14. Mao X, Zhou L, Tey SK, Ma APY, Yeung CLS, Ng TH, *et al.* Tumour extracellular vesicle-derived Complement Factor H promotes tumorigenesis and metastasis by inhibiting complement-dependent cytotoxicity of tumour cells. J Extracell Vesicles 2020;10(1):e12031 doi 10.1002/jev2.12031.
15. Saxena R, Bushey R, Campa M, Gottlin E, Guo J, Patz E, *et al.* Creation of a Favorable Antitumor Microenvironment by the Anti-Complement Factor H Antibody GT103 (Preprint) **2022** https://doi.org/10.21203/rs.3.rs-2001920/v1.
16. Kamen L, Myneni S, Langsdorf C, Kho E, Ordonia B, Thakurta T, *et al.* A novel method for determining antibody-dependent cellular phagocytosis. Journal of immunological methods 2019;468:55–60 doi 10.1016/j.jim.2019.03.001.
17. Kataoka H, Kono H, Patel Z, Kimura Y, Rock KL. Evaluation of the contribution of multiple DAMPs and DAMP receptors in cell death-induced sterile inflammatory responses. PLoS One 2014;9(8):e104741 doi 10.1371/journal.pone.0104741.

18. Chao MP, Jaiswal S, Weissman-Tsukamoto R, Alizadeh AA, Gentles AJ, Volkmer J, *et al.* Calreticulin is the dominant pro-phagocytic signal on multiple human cancers and is counterbalanced by CD47. Sci Transl Med 2010;2(63):63ra94 doi 10.1126/scitranslmed.3001375.
19. Obeid M, Tesniere A, Ghiringhelli F, Fimia GM, Apetoh L, Perfettini JL, *et al.* Calreticulin exposure dictates the immunogenicity of cancer cell death. Nat Med 2007;13(1):54–61 doi 10.1038/nm1523.
20. Carroll MC, Isenman DE. Regulation of humoral immunity by complement. Immunity 2012;37(2):199–207 doi 10.1016/j.immuni.2012.08.002.
21. Clemenza L, Isenman DE. Structure-guided identification of C3d residues essential for its binding to complement receptor 2 (CD21). J Immunol 2000;165(7):3839–48 doi 10.4049/jimmunol.165.7.3839.
22. Kalli KR, Ahearn JM, Fearon DT. Interaction of iC3b with recombinant isotypic and chimeric forms of CR2. J Immunol 1991;147(2):590–4.
23. Lyubchenko T, dal Porto J, Cambier JC, Holers VM. Coligation of the B cell receptor with complement receptor type 2 (CR2/CD21) using its natural ligand C3dg: activation without engagement of an inhibitory signaling pathway. J Immunol 2005;174(6):3264–72 doi 10.4049/jimmunol.174.6.3264.
24. Nagar B, Jones RG, Diefenbach RJ, Isenman DE, Rini JM. X-ray crystal structure of C3d: a C3 fragment and ligand for complement receptor 2. Science 1998;280(5367):1277–81 doi 10.1126/science.280.5367.1277.
25. Merle NS, Noe R, Halbwachs-Mecarelli L, Fremeaux-Bacchi V, Roumenina LT. Complement System Part II: Role in Immunity. Front Immunol 2015;6:257 doi 10.3389/fimmu.2015.00257.
26. Sarma JV, Ward PA. The complement system. Cell Tissue Res 2011;343(1):227–35 doi 10.1007/s00441-010-1034-0.
27. Bushey RT, Gottlin EB, Campa MJ, Patz EF, Jr. Complement factor H protects tumor cell-derived exosomes from complement-dependent lysis and phagocytosis. PLoS One 2021;16(6):e0252577 doi 10.1371/journal.pone.0252577.
28. Ackermann JA, Nys J, Schweighoffer E, McCleary S, Smithers N, Tybulewicz VL. Syk tyrosine kinase is critical for B cell antibody responses and memory B cell survival. J Immunol 2015;194(10):4650–6 doi 10.4049/jimmunol.1500461.
29. Dunkelberger JR, Song WC. Complement and its role in innate and adaptive immune responses. Cell Res 2010;20(1):34–50 doi 10.1038/cr.2009.139.
30. Carroll MC. Complement and humoral immunity. Vaccine 2008;26 Suppl 8:I28-33 doi 10.1016/j.vaccine.2008.11.022.
31. Ferreira VP, Pangburn MK, Cortes C. Complement control protein factor H: the good, the bad, and the inadequate. Mol Immunol 2010;47(13):2187–97 doi 10.1016/j.molimm.2010.05.007.
32. Parente R, Clark SJ, Inforzato A, Day AJ. Complement factor H in host defense and immune evasion. Cell Mol Life Sci 2017;74(9):1605–24 doi 10.1007/s00018-016-2418-4.
33. Ajona D, Castano Z, Garayoa M, Zudaire E, Pajares MJ, Martinez A, *et al.* Expression of complement factor H by lung cancer cells: effects on the activation of the alternative pathway of complement.

Cancer Res 2004;64(17):6310–8.

34. Smolag KI, Mueni CM, Leandersson K, Jirstrom K, Hagerling C, Morgelin M, *et al.* Complement inhibitor factor H expressed by breast cancer cells differentiates CD14(+) human monocytes into immunosuppressive macrophages. Oncoimmunology 2020;9(1):1731135 doi 10.1080/2162402X.2020.1731135.
35. Junnikkala S, Hakulinen J, Jarva H, Manuelian T, Bjorge L, Butzow R, *et al.* Secretion of soluble complement inhibitors factor H and factor H-like protein (FHL-1) by ovarian tumour cells. British journal of cancer 2002;87(10):1119–27.
36. Fishelson Z, Kirschfink M. Complement C5b-9 and Cancer: Mechanisms of Cell Damage, Cancer Counteractions, and Approaches for Intervention. Frontiers in immunology 2019;10:752 doi 10.3389/fimmu.2019.00752.
37. Lusthaus M, Mazkereth N, Donin N, Fishelson Z. Receptor-Interacting Protein Kinases 1 and 3, and Mixed Lineage Kinase Domain-Like Protein Are Activated by Sublytic Complement and Participate in Complement-Dependent Cytotoxicity. Frontiers in immunology 2018;9:306 doi 10.3389/fimmu.2018.00306.
38. Ziporen L, Donin N, Shmushkovich T, Gross A, Fishelson Z. Programmed necrotic cell death induced by complement involves a Bid-dependent pathway. J Immunol 2009;182(1):515–21.
39. Vandenabeele P, Vandecasteele K, Bachert C, Krysko O, Krysko DV. Immunogenic Apoptotic Cell Death and Anticancer Immunity. Adv Exp Med Biol 2016;930:133–49 doi 10.1007/978-3-319-39406-0_6.
40. Sprooten J, De Wijngaert P, Vanmeerbeerk I, Martin S, Vangheluwe P, Schlenner S, *et al.* Necroptosis in Immuno-Oncology and Cancer Immunotherapy. Cells 2020;9(8) doi 10.3390/cells9081823.
41. Zitvogel L, Kepp O, Senovilla L, Menger L, Chaput N, Kroemer G. Immunogenic tumor cell death for optimal anticancer therapy: the calreticulin exposure pathway. Clin Cancer Res 2010;16(12):3100–4 doi 10.1158/1078 – 0432.CCR-09-2891.
42. Lu Y, Zhao Q, Liao JY, Song E, Xia Q, Pan J, *et al.* Complement Signals Determine Opposite Effects of B Cells in Chemotherapy-Induced Immunity. Cell 2020;180(6):1081-97 e24 doi 10.1016/j.cell.2020.02.015.

Declarations

Financial Support

This work was funded by the Department of Defense through the Lung Cancer Research Program under Award No. W81XWH-19-1-0342 to EFP and YWH.

*Corresponding Author

Edward F. Patz, Jr., Box 3808, Duke University Medical Center, Durham, NC 27710, Tel: +1 919-684-7311, patz0002@mc.duke.edu

Conflicts of Interest

EFP is a Founder, Board Member, and the CEO of Grid Therapeutics, LLC. MJC and EBG are Founders of Grid Therapeutics, LLC.

Figures

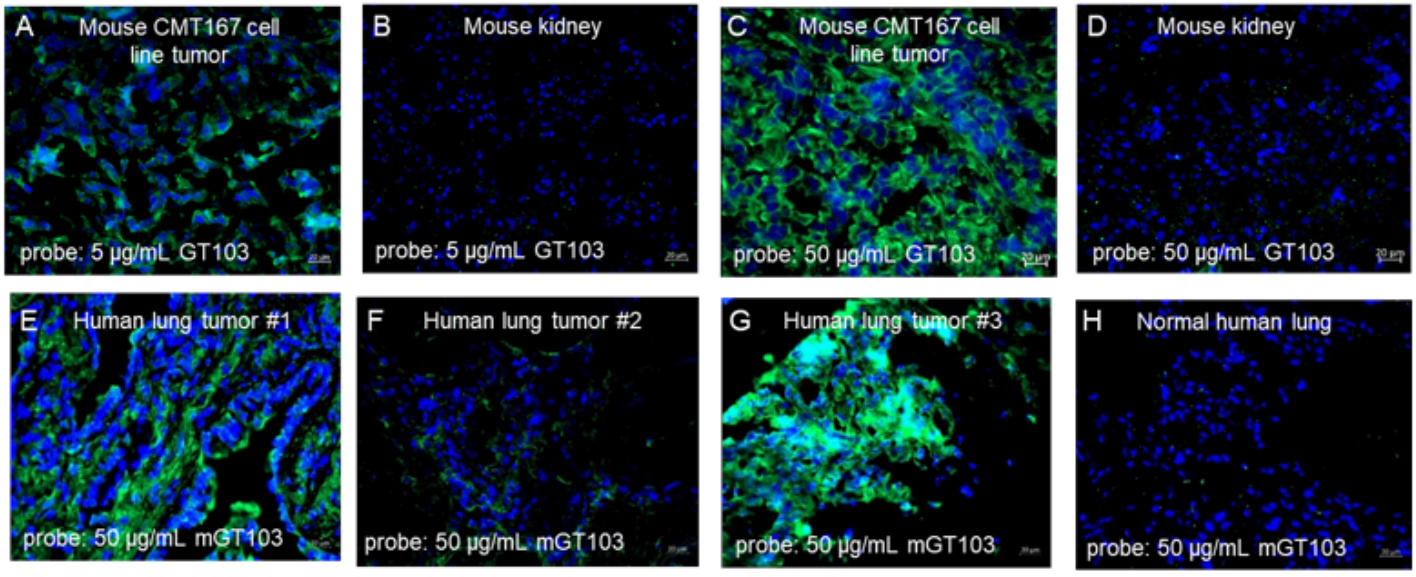

I

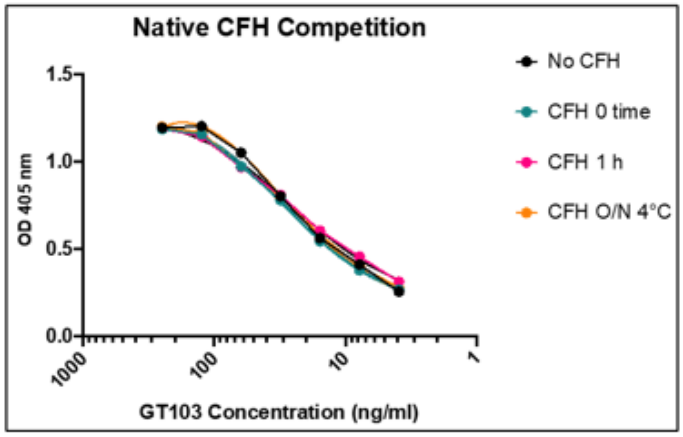

J

µg/ml GT103	µg/ml CFH	CFH/GT103 molar ratio
0.25	50	200
0.125	50	400
0.0625	50	800
0.03125	50	1600
0.015625	50	3200
0.0078125	50	6400
0.00390625	50	12800

Figure 1

Tumor specificity of GT103. (A-H) Immunofluorescence of tumor and normal tissues probed with GT103. To avoid unwanted cross-reaction of secondary antibodies with IgG in tissues, mouse tissues were probed with human GT103 and human tissues with mGT103. **(A-D)** GT103 binding to mouse tissue.

Human GT103 binding to CMT167 mouse cell line tumors was observed at **(A)** 5 µg/ml or **(C)** 50 µg/ml GT103, while no binding was observed in normal mouse kidney at the same GT103 concentrations at **(B)** 5 µg/ml or **(D)** 50 µg/ml. Representative images are shown; multiple tumor and kidney samples were probed with GT103 and identical results were observed. **(E-H)** mGT103 binding to human tissue. Thirty-three human lung tumor spots on a TMA were probed with mGT103 at 50 µg/ml and three representative images showing variability in staining are shown **(E-G)**. No fluorescence was detected in multiple normal human lung tissue samples probed with mGT103 at the same concentration; a representative image is shown in **(H)**. No fluorescence was observed for any samples with secondary antibody in the absence of GT103 (data not shown). **(I)** ELISA data showing the inability of soluble CFH to interfere with the interaction of GT103 with immobilized epitope peptide. **(J)** Concentrations of GT103 and CFH used in the ELISA.

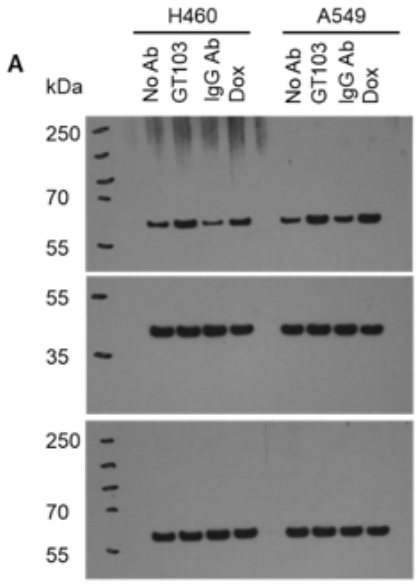

B

Cell Line	Treatment	Normalized Relative Intensity
H460	No antibody	1
	GT103	1.92
	IgG3 control	0.71
	Doxorubicin	1.73
A549	No antibody	1
	GT103	2.23
	IgG3 control	1.14
	Doxorubicin	2.34

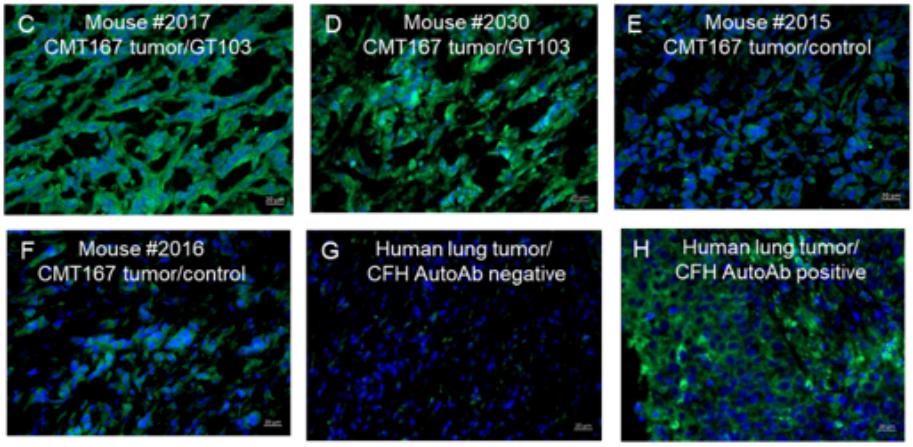

C-H tumor sections probed with anti-calreticulin antibody

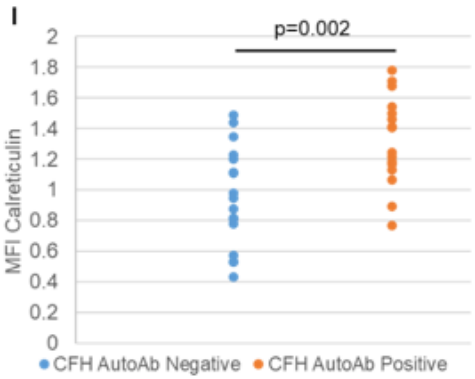

Figure 2

Plasma membrane expression of calreticulin increases following GT103 treatment. (A) Anti-calreticulin western blots of plasma membrane and total lysates of tumor cells treated *in vitro* with GT103 or control. H460 and A549 cells were treated with GT103 or control IgG in the presence of NHS, or with doxorubicin as a positive control. Plasma membranes or whole cell lysates were prepared and subjected to western blot analysis. Top panel: Plasma membrane blot probed with anti-calreticulin antibody; Middle panel:

Same blot stripped and probed with anti-beta-actin antibody (loading control); Bottom panel: Whole lysate blot probed with anti-calreticulin antibody. **(B)** Intensity of the calreticulin band normalized to beta-actin and expressed relative to a no antibody control. **(C-H)** Immunofluorescence for calreticulin in tumors of GT103- or control treated mice or tumors of anti-CFH autoantibody-positive and -negative NSCLC patients. CMT167 tumor sections from GT103-treated **(C,D)** or control-treated **(E,F)** mice were probed with anti-calreticulin and secondary antibodies. Human lung tumor sections from anti-CFH autobody-negative or -positive patients were similarly stained; two such sections are shown in panels **(G,H)**. Human lung tumor samples on a TMA were also stained for calreticulin, images of two fields were captured for each of the 33 spots stained with calreticulin antibody, and the mean MFI of calreticulin was determined. Variability in fluorescence between samples is represented in panel **(I)**. There was a significant difference in calreticulin MFI between anti-CFH autoantibody-positive and -negative samples (mean MFI of positive group = 1.32; mean MFI of negative group = 0.92; p=0.002). No background fluorescence was observed for mouse or human samples with secondary antibody alone.

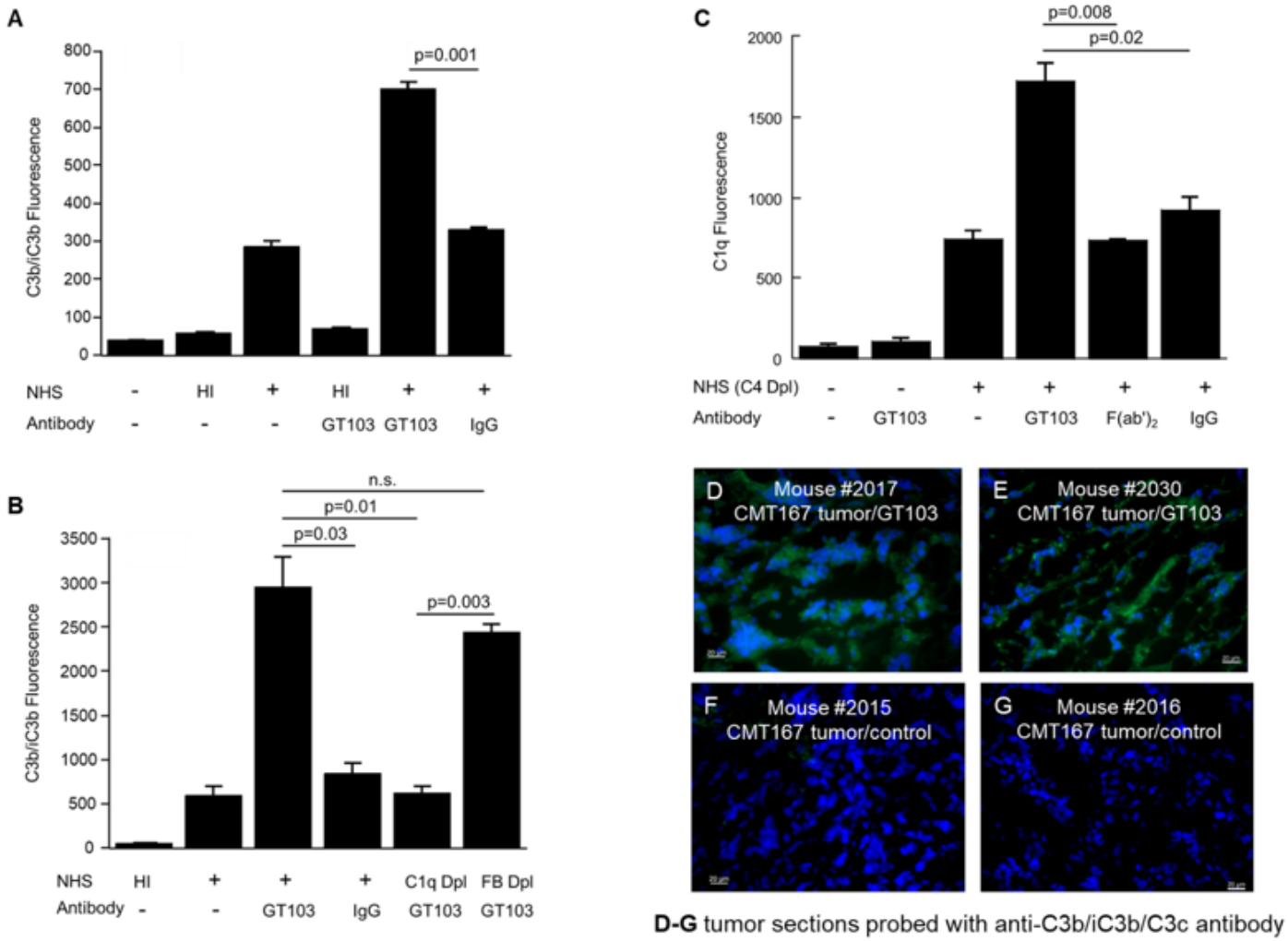

D-G tumor sections probed with anti-C3b/iC3b/C3c antibody

Figure 3

GT103 causes deposition of complement split products on tumor cells *in vitro* and *in vivo* via the classical complement pathway. (A-B) C3b/iC3b deposition on tumor cells. **(A)** A549 and **(B)** H460 human lung cancer cells were treated *in vitro* with GT103 or IgG in the presence of NHS or heat-inactivated (HI) NHS. In **(B)**, cells were also incubated with antibodies in the presence of C1q-depleted or Factor B-depleted NHS. C3b/iC3b binding to cells was measured by flow cytometry. Each condition was run in triplicate, and the data are shown as mean C3b/iC3b fluorescence ± SD. **(C)** C1q deposition on H460 lung cancer cells. Cells were treated with GT103, the $F(ab')_2$ of GT103, or IgG in C4-depleted NHS (used to supply complement but not allow cell lysis). C1q binding was measured by flow cytometry. Each condition was run in triplicate, and the data are shown as C1q fluorescence ± SD. **(D-G)** CMT167 tumors from mouse studies were analyzed for C3 fragments (C3b/iC3b/C3c) by immunofluorescence. GT103 treated CMT167 tumors **(D-E)** were compared to control treated CMT167 tumors **(F-G)**.

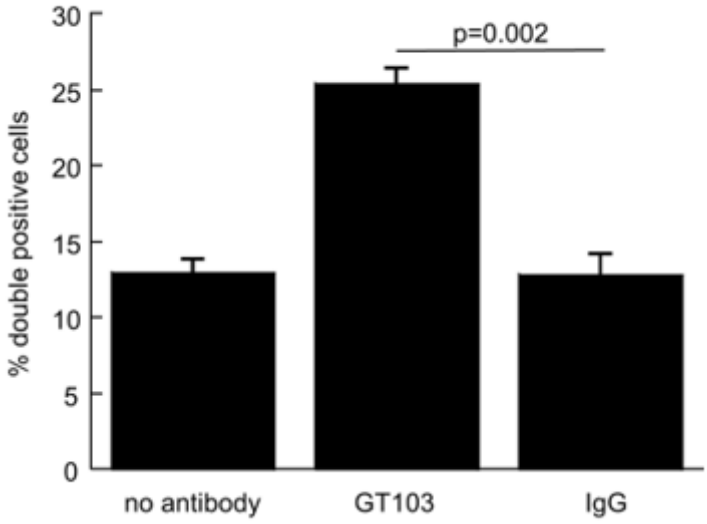

Figure 4

GT103 causes increased macrophage-mediated ADCP of H460 lung cancer cells. Macrophages and tumor cells were labeled with different fluorophores and either no antibody, human GT103, or matched IgG control antibody were added at 250 µg/ml. After coincubation of macrophages and tumor cells, double positive cells were isolated by flow cytometry. Each condition was performed in triplicate.

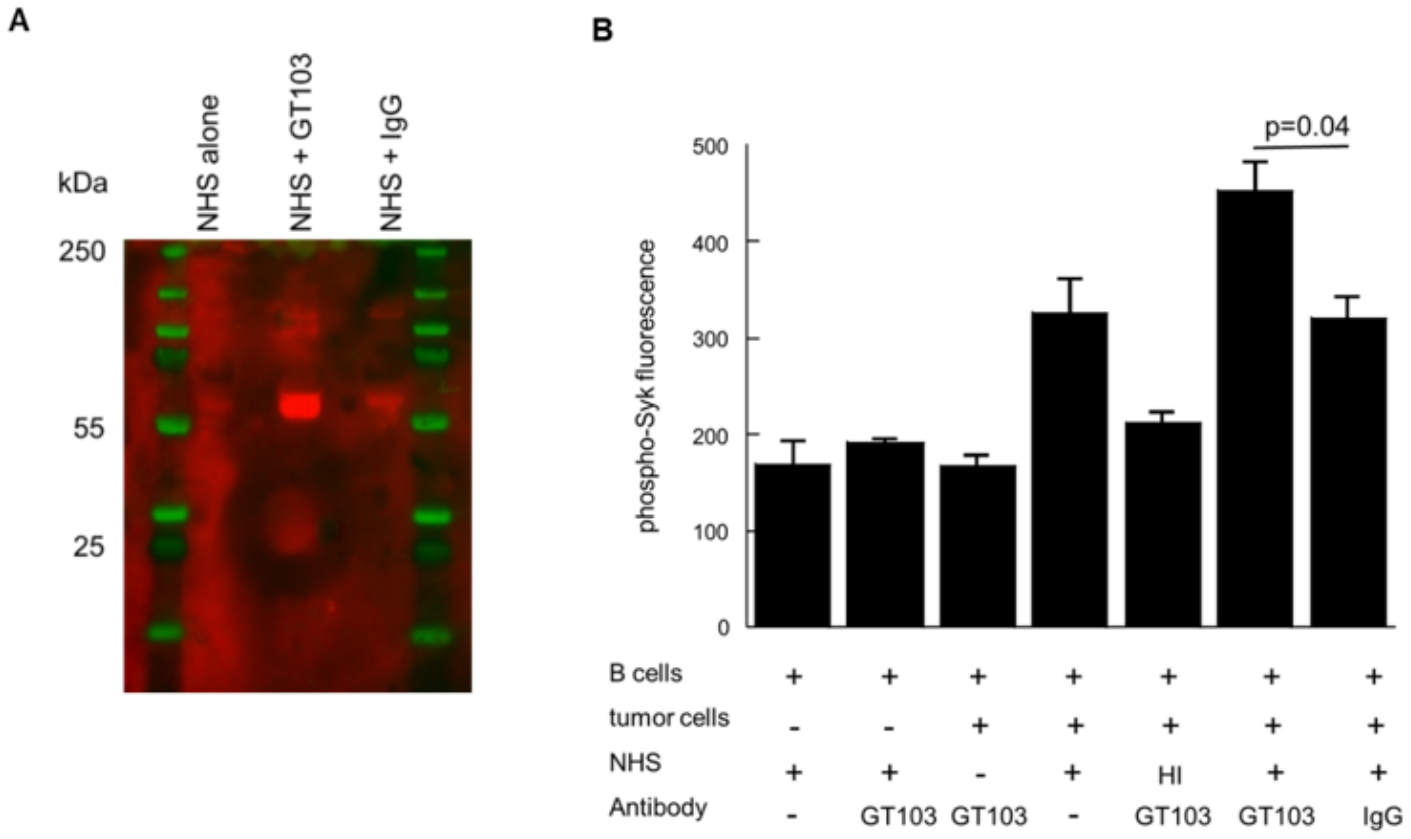

Figure 5

GT103 induces phosphorylation of Syk kinase in B cells co-cultured with tumor cells. H460 lung cancer cells were treated with GT103 or IgG in the presence of NHS and then co-cultured with B cells for 24 hrs. **(A)** Lysates of the cell mixtures were probed with an antibody against phosphorylated Syk by immunoblot. **(B)** The same experimental setup was performed, with the addition of controls in which B cells were incubated in the absence of tumor cells, and B cells were permeabilized, gated and stained for phosphorylated Syk by flow cytometry. Each condition was run in duplicate, and phospho-Syk fluorescence is represented as mean ± SD.

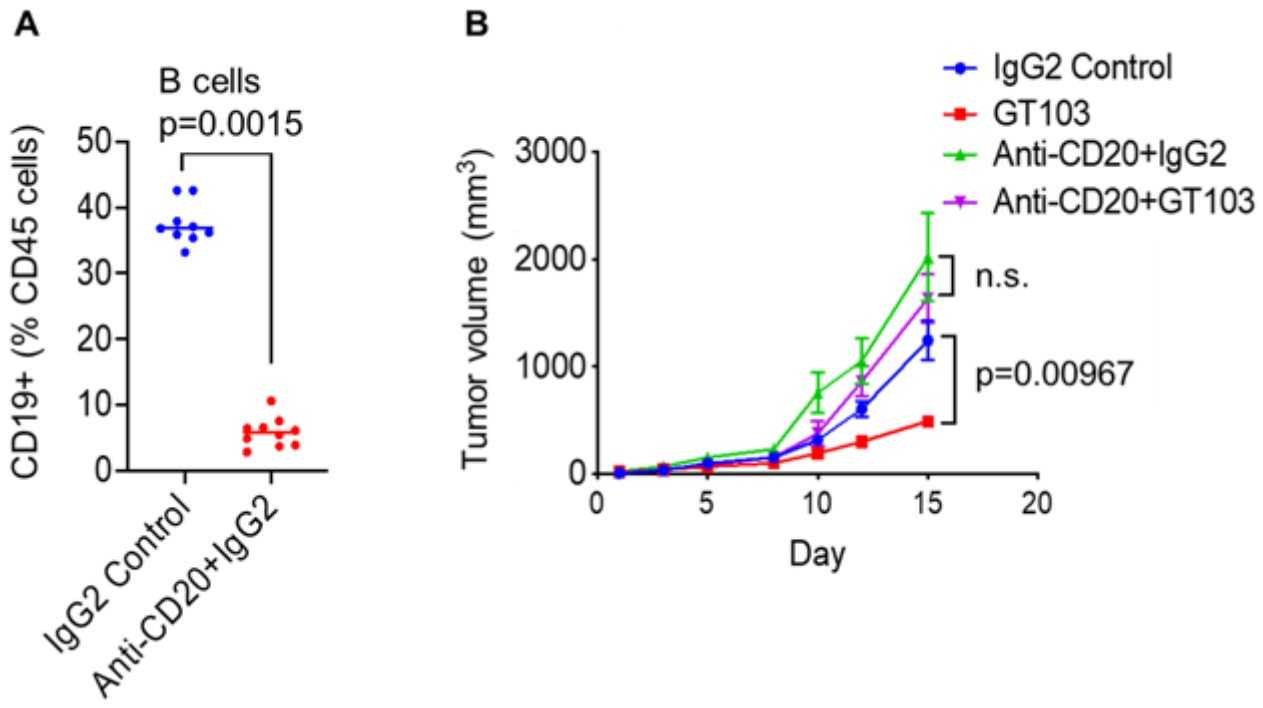

Figure 6

Inhibition of CMT167 tumor growth by GT103 requires B cells. Ten six to eight week old C57BL/6 mice were injected with anti-CD20 three days prior to tumor inoculation to deplete B cells. The 10 B cell-depleted and 10 nondepleted C57BL/6 mice were inoculated s.c. with CMT167 cells. When tumors were palpable, mice in each group were dosed three times a week with control IgG2 or GT103 i.p. Tumor volume was plotted as mean ± SEM for n=3-5 for each treatment group.